

## Photolysis of Heptanal

Suzanne E. Paulson,\* De-Ling Liu,<sup>†</sup> and Grazyna E. Orzechowska<sup>†</sup>

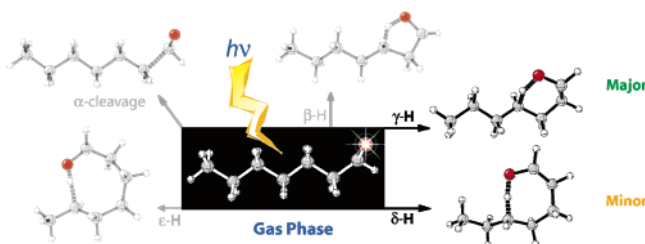
Department of Atmospheric and Oceanic Sciences, University of California,  
Los Angeles, California 90095-1565

Luis M. Campos and K. N. Houk

Department of Chemistry and Biochemistry, University of California, Los Angeles, California 90095-1565

paulson@atmos.ucla.edu

Received March 18, 2006



Photolysis of heptanal is investigated from an experimental and theoretical point of view. Photoexcited heptanal is believed to undergo rapid intersystem crossing to the triplet manifold and from there undergoes internal H-abstraction to form biradical intermediates. The favored  $\gamma$ -H abstraction pathway can cyclize or cleave to 1-pentene and hydroxyethene, which tautomerizes to acetaldehyde. Yields of 1-pentene and acetaldehyde were measured at  $62 \pm 7\%$  and  $63 \pm 7\%$ , respectively, relative to photolyzed heptanal. Additionally, small quantities of hexanal and hexanol were observed. On the basis of combined experimental and theoretical evidence, the remaining heptanal photolysis proceeds to form an estimated 10% HCO + hexyl radical and 30% cyclic alcohols, particularly 2-propyl cyclobutanol and 2-ethyl cyclopentanol.

### Introduction

Straight-chain aldehydes, including heptanal, are ubiquitous in the Earth's boundary layer. At remote sites, long-chain aldehydes are frequently among the most prominent organics observed. Concentrations typically fall in the mid parts per trillion to several parts per billion range for clean continental, coastal, and urban air.<sup>1,2</sup> Heptanal has many natural sources, including trees and grasses, and emission rates can be comparable to terpene emission rates.<sup>3,4</sup> Heptanal is also produced by most if not all combustion sources, including motor vehicles, wood burning, and cooking.<sup>5</sup> Finally, heptanal is generated

photochemically via ozone reactions with long-chain alkenes such as 1-octene.<sup>6</sup>

Aldehydes are an important source of chain-initiating radicals throughout the Earth's troposphere,<sup>7</sup> via their Norrish type I photodecomposition channel ( $\alpha$ -cleavage, a, Scheme 1). Photolysis of larger aldehydes appears to produce fewer radicals in favor of cyclization (b or c) or cleavage to an alkene and alcohol (b, the Norrish type II cleavage). Aldehydes also appear to be key components of secondary organic aerosol formation, contributing to polymerization reactions,<sup>8,9</sup> although this is debated.<sup>10</sup>

<sup>†</sup> Now at the Jet Propulsion Laboratory, Pasadena, CA 91109.

(1) Zielinska, B.; Fujita, E. M. *Atmos. Environ.* **2003**, *37*, S171–S180.  
(2) Grossmann, D.; Moortgat, G.; Kibler, M.; Schlomski, S.; Bachmann, K.; Alicke, B.; Geyer, A.; Platt, U.; Hammer, M.; Vogel, B.; Mihelcic, D.; Hofzumahaus, A.; Holland, F.; Volz-Thomas, A. *J. Geophys. Res.* **2003**, *108* (D4): Art. No. 8250.

(3) Owen, S.; Boissard, C.; Street, R. A.; Duckham, S. C.; Csiky, O.; Hewitt, C. N. *Atmos. Environ.* **1997**, *31*, 101–117.

(4) Kirstine, W.; Galbally, I.; Ye, Y. R.; Hooper, M. *J. Geophys. Res.* – Atmos. **1998**, *103*, 10605–10619.

(5) Schauer, J. J.; Kleeman, M. J.; Cass, G. R.; Simoneit, B. R. T. *Environ. Sci. Technol.* **2002**, *36*, 567–575.

(6) Paulson, S. E.; Chung, M. Y.; Hasson, A. S. *J. Phys. Chem. A* **1999**, *103*, 8125–8138.

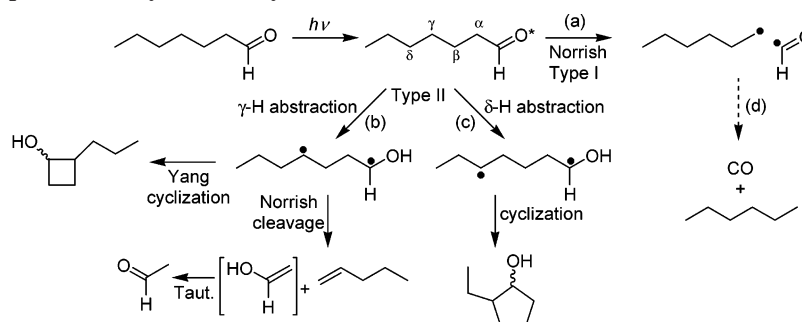
(7) Paulson, S. E.; Orlando, J. J. *Geophys. Res. Lett.* **1996**, *23*, 3727–3730.

(8) Ziemann, P. *J. Faraday Discuss.* **2005**, *130*, 469–490.

(9) Tolocka, M. P.; Jang, M.; Ginter, J. M.; Cox, F. J.; Kamens, R. M.; Johnston, M. V. *Environ. Sci. Technol.* **2004**, *38*, 1428–1434.

(10) Kroll, J. H.; Ng, N. L.; Murphy, S. M.; Varutbangkul, V.; Flagan, R. C.; Seinfeld, J. H. *J. Geophys. Res.* – Atmos. **2005**, *110*, Art. No. D23207.

## SCHEME 1. Possible Heptanal Photolysis Pathways



The smallest members of the aldehyde family, formaldehyde, acetaldehyde, and propanal, have been studied extensively. Aldehydes with four or more carbons have additional reaction pathways available to them but have been investigated only by a handful of studies,<sup>11–14</sup> and product yields vary widely among studies.

Here, we provide results of a combined experimental and theoretical investigation of heptanal photolysis. Products of photolysis initiated with ultraviolet (UV) lamps have been measured using gas chromatography with flame ionization and mass spectral detectors (GC-FID and GC-MS), using on-column injection, solid-phase microextraction (SPME), and derivatization to introduce samples. Theoretical investigations of the reactions of the triplet aldehyde that results from photoexcitation were performed using density functional theory.

## Mechanism

Heptanal, like other alkyl aldehydes, exhibits a weak, symmetry forbidden  $n-\pi^*$  transition in the 240–360 nm region,<sup>13,14</sup> overlapping with near UV solar wavelengths that penetrate into the upper troposphere and, to a lesser degree, into the Earth's surface. Although H-abstraction can take place from the singlet state, the very fast rate of intersystem crossing of aldehydes (ca.  $10^8 \text{ s}^{-1}$ )<sup>15</sup> to the triplet state is more likely to be the predominant path, followed by H-abstraction from the triplet state.

Heptanal photolysis is thought to proceed via several pathways, illustrated in Scheme 1. These include (a) Norrish type I cleavage leading to *n*-hexyl and HCO radicals and several cyclization pathways involving a  $\beta$ -,  $\gamma$ -,  $\delta$ -, or  $\epsilon$ -hydrogen abstraction; (b) the  $\gamma$ -H abstraction leading to a biradical that can undergo Norrish II cleavage to 1-pentene and hydroxyethene (which tautomerizes to acetaldehyde) or can undergo a Yang cyclization to 2-propylcyclobutanol; (c) the  $\delta$ -H abstraction leading to a biradical that can undergo cyclization to 2-ethylcyclopentanol; and (d) decarbonylation to CO and hexane which have been suggested as products of heptanal photolysis, analogous to other aldehydes (e.g., Tang and Zhu<sup>14</sup>). We were not able to determine a plausible mechanism leading to decarbonylation (Scheme 1, d, see below). Results of Tang and Zhu's studies performed at multiple wavelengths in the 280–330 range indicate that the Norrish I channel producing HCO

has only a slight dependence on wavelength,<sup>14</sup> consistent with the notion that pathways a–c are enthalpically accessible throughout the range of absorption wavelengths.

We focused on the triplet state path, which according to the fast rate of intersystem crossing previously mentioned is most likely to be a heavily populated state. Long-chain ketones also exhibit photochemistry similar to long-chain aldehydes. De Feyter et al.<sup>16</sup> have studied the femtosecond dynamics of ketones with  $\gamma$ -hydrogens. It is interesting to note that their studies focused on the higher-energy singlet state reaction and found that intersystem crossing competed with reactivity in the singlet manifold. Upon generation of the singlet biradical, cyclization and cleavage took place without noticeable energetic barriers. In their studies, they also reported calculations along the singlet ground-state manifold for the Norrish cleavage and Yang cyclization of the biradical generated after  $\gamma$ -H abstraction. In essence, such a biradical is postulated to react similarly to the singlet 1,4-biradical generated after intersystem crossing (ISC) of the triplet 1,4-biradical from heptanal (this study). Wagner has noted that cyclization and cleavage reactions may occur from both the singlet and triplet states. That is, because the geometric changes are similar for product formation and ISC, the triplet biradical can react to form products without reverting to the singlet state before product formation.<sup>17,18</sup>

## Results

**Measurements.** UV photolysis of heptanal resulted in several products, dominated by 1-pentene, acetaldehyde, and hexanal, together with trace quantities of hexanol and several unidentified products, a few with yields of up to about 7%. Positive identities of the first four products were established by comparing retention times and ionization fingerprints in GC-MS to authentic standards and the NIST mass spectral library. The measured photolysis yields (relative to reacted heptanal) of acetaldehyde, 1-pentene, and *n*-hexanal were  $63 \pm 6\%$ ,  $62 \pm 7\%$ , and  $7 \pm 3\%$ , respectively (Figure 1 and Table 1). A small correction was made to the acetaldehyde data to account for its photolysis. 1-Hexanol was also observed in both the SPME/GC-MS and GC-FID samples, but with a yield of less than 0.5%. No peak was observed at the retention time of *n*-hexane, which was established by authentic standards and its Kovats index. Two products (unknowns indicated in Table 1) with yields of around 7% each elute after *n*-heptanal and in approximately

(11) Chen, Y. Q.; Zhu, L.; Francisco, J. S. *J. Phys. Chem. A* **2002**, *106*, 7755–7763.

(12) Tadić, J.; Juranic, I.; Moortgat, G. K. *Molecules* **2001**, *6*, 287–299.

(13) Tadić, J. M.; Juranic, I. O.; Moortgat, G. K. *J. Chem. Soc., Perkin Trans. 2* **2002**, 135–140.

(14) Tang, Y.; Zhu, L. *J. Phys. Chem. A* **2004**, *108*, 8307–8316.

(15) Hansen, D. A.; Lee, E. K. *J. Chem. Phys.* **1975**, *63*, 3272–3277.

(16) De Feyter, S.; Diau, E. W.-G.; Zewail, A. H. *Angew. Chem., Int. Ed.* **2000**, *39*, 260–263.

(17) Wagner, P. J. In *CRC Handbook of Organic Photochemistry and Photobiology*, 2nd ed.; Horspool, W. M., Lenci, F., Eds.; CRC Press: New York, 2004; Chapter 58.

(18) Michl, J. *J. Am. Chem. Soc.* **1996**, *118*, 3568–3579.

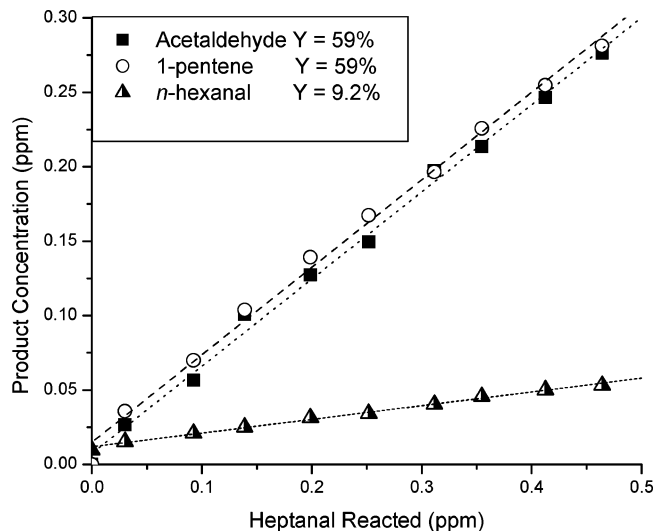


**FIGURE 1.** Products from UV photolysis of heptanal in air at atmospheric pressure, experiment 4. The initial heptanal concentration was 2.6 ppm.

the correct location for C<sub>7</sub> cyclic alcohols that are expected from the  $\gamma$ - and  $\delta$ -H abstraction pathways. The identity of these products could not be confirmed by SPME/GC-MS, or from their Kovats indices. Products may not have been successfully recovered from the SPME fiber, either because they decomposed or were retained by the SPME fiber. Further, authentic standards and index data are not available for these compounds.

**Theoretical.** The optimized structures (triplet heptanal, transition structures, and selected biradicals) of importance for hydrogen transfer and  $\alpha$ -cleavage are shown in Scheme 2, along with the zero-point energy inclusive barrier heights (in kcal/mol). In comparing the feasibility of the carbonyl oxygen to extract a  $\beta$ -,  $\gamma$ -,  $\delta$ -, or  $\epsilon$ -hydrogen, one can clearly see that the highest barrier heights correspond to the formation of a five- and an eight-membered ring ( $\beta$ - and  $\epsilon$ -H). Furthermore,  $\alpha$ -cleavage is also a high-energy process, relative to  $\gamma$ - and  $\delta$ -hydrogen abstraction, requiring 11 kcal/mol to overcome the barrier height. Although  $\gamma$ -hydrogen abstraction has the lowest barrier height (6.9 kcal/mol), the transition structure for  $\delta$ -H abstraction lies only 0.8 kcal/mol above the  $\gamma$ -H channel. Kinetically, transition state theory predicts that the biradicals arising from  $\gamma$ -H and  $\delta$ -H abstraction will form in  $\sim 80\%$  and  $\sim 20\%$  yields, respectively, whereas trace amounts of the  $\alpha$ -cleavage may be observed. The generation of both biradical intermediates  $^3\text{BR-}\gamma$  and  $^3\text{BR-}\delta$  is slightly endothermic, allowing for a feasibly reversible path that can potentially explore other channels such as the Norrish I. Following the formation of the triplet biradicals,  $^3\text{BR-}\gamma$  and  $^3\text{BR-}\delta$ , cyclization and/or cleavage may be accessed.<sup>16–18</sup> Note that the percentages correspond to formation of the biradicals and not the products. The pathways of  $^3\text{BR-}\gamma$  include cleavage to 1-pentene and hydroxyethylene and cyclobutanol formation (see Scheme 1).

We also calculated the relative energies of the ground-state products following biradicals  $^3\text{BR-}\gamma$  and  $^3\text{BR-}\delta$  (see Scheme 1). The relative energies of the *cis*- and *trans*-cyclopentanols (from cyclization of  $^3\text{BR-}\delta$ ) are  $-65.7$  and  $-65.9$  kcal/mol, respectively, and cleavage of the  $^3\text{BR-}\gamma$  yields 1-pentene and hydroxyethylene at a relative energy of  $-35.5$  kcal/mol. Furthermore, the cyclization of  $^3\text{BR-}\gamma$  would yield the *cis*- and *trans*-cyclobutanols at relative energies of  $-48.8$  and  $-51.5$

kcal/mol, respectively. Such values are relatively similar to the values of the singlet biradicals obtained for the  $\gamma$ -H abstraction of 2-pentanone.<sup>16</sup>

## Discussion

Table 2 summarizes the theoretical and experimental results of this work, together with two earlier investigations of heptanal photolysis.

**Norrish I Channel.** Theory suggests that the Norrish I cleavage, which dominates the photolysis products from small aldehydes, should be essentially shut down for heptanal in the triplet state. This is due to the competing type II channels that have barrier heights that are lower by at least 3.5 kcal/mol, leading to hydrogen abstraction products. It may be possible, however, that the Norrish I channel may be accessed through the singlet state, before intersystem crossing to the competing triplet state, as it has been previously observed for ketones similar to the case of heptanal.<sup>16,19</sup> Alternatively, the reversibility of the biradicals generated may allow for the triplet state to access this channel leading to the hexyl and HCO radicals at a relative energy of 7.4 kcal/mol.

In our experiments, we observed formation of hexanol and hexanal, which could arise from the hexyl radical produced by the Norrish I channel. Pathways leading to these products are shown in Scheme 3: disproportionation of C<sub>6</sub>H<sub>13</sub>OO (pathway a) produces both hexanol and hexanal, and the self-reaction of C<sub>6</sub>H<sub>13</sub>OO producing two primary hexyloxyl radicals (b), followed by the reaction of the hexyloxyl radical with O<sub>2</sub> (e), generates hexanal. Little hexanol and hexanol are expected however, as the self-reaction of C<sub>6</sub>H<sub>13</sub>OO, radical formation (b), is expected to dominate disproportionation (a) by perhaps a factor of 5.<sup>20,21</sup> Further, a substantial body of literature indicates that the hexyloxyl radical isomerization (d) should be favored over reaction with O<sub>2</sub> (e),<sup>20,21</sup> such that only about 4% of hexyloxyl radicals should eventually generate hexanal in 1 atm of air (calculated with FACSIMILE). Given that products other than the hexyl radical account for most of the heptanal photolyzed, it is difficult to rationalize such a high yield of hexanal. The observed trace quantities of hexanol, on the other hand, are consistent with a moderate yield of hexyl radicals, in the neighborhood of 10% or less.

Norrish I cleavage was monitored with CO and HCO by Tadić et al.<sup>13</sup> and Tang and Zhu,<sup>14</sup> respectively. Tang and Zhu<sup>14</sup> measured the HCO yield at discrete wavelengths and found that HCO formation varied from 0.10 to 0.15 over the wavelength range 305–320 nm. Tadić et al.<sup>13</sup> estimated the  $\alpha$ -cleavage channel at 10% after correcting the CO they observed for secondary reactions that also generate CO, which accounted for nearly half of the CO by the end of their experiments. Interpretation of the HCO observations from high-concentration (1700–13 000 ppm) cavity ring down experiments<sup>14</sup> requires a kinetics model, increasing the uncertainty in this method.

Taken together, the experimental evidence indicates that the Norrish I cleavage accounts for  $\sim 10\%$  of heptanal photolysis products. Although the theoretical explanation with respect to the triplet state is not entirely clear,  $\alpha$ -cleavage may be possibly accessed from the singlet state.

(19) Diau, E. W.-G.; Kötting, C.; Zewail, A. H. *ChemPhysChem* **2001**, *2*, 273–293.

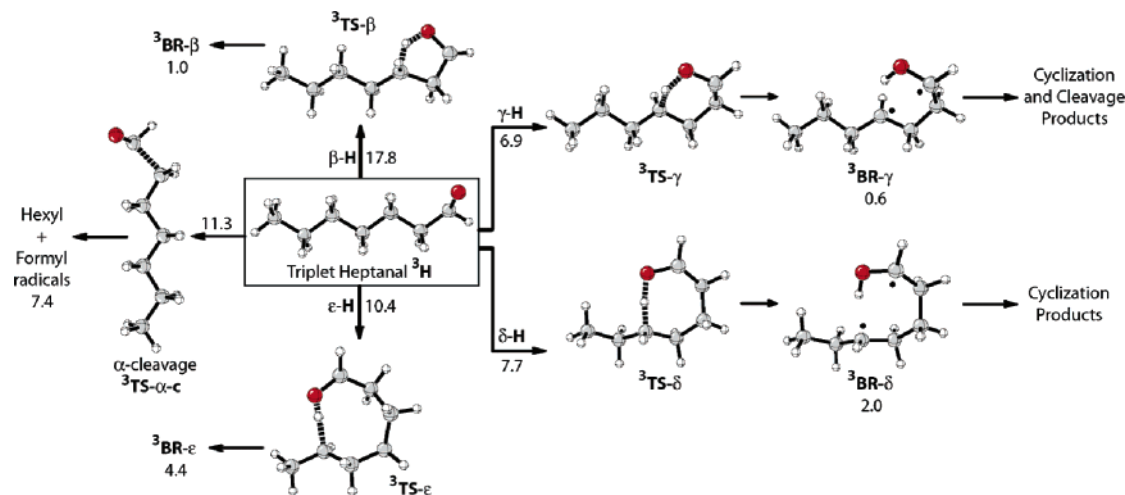
(20) Atkinson, R.; Arey, J. *Chem. Rev.* **2003**, *103*, 4605–4638.

(21) Orlando, J. J.; Tyndall, G. S.; Apel, E. C.; Riemer, D. D.; Paulson, S. E. *Int. J. Chem. Kinet.* **2003**, *35*, 334–353.

TABLE 1. Product Yields for Heptanal Photolysis Experiments

| experiment | initial heptanal (ppm) | product yields (%) |              |         |                      |                      |
|------------|------------------------|--------------------|--------------|---------|----------------------|----------------------|
|            |                        | 1-pentene          | acetaldehyde | hexanal | Unk. 1 <sup>a</sup>  | Unk. 2 <sup>a</sup>  |
| 1          | 2.1                    | 58                 | 55           | 5.4     | 5.1                  | 5.6                  |
| 2          | 2.9                    | 70                 | 71           | 5.3     | 5.4                  | 6.6                  |
| 3          | 2.5                    | 64                 | 64           | 4.3     | 6.7                  | 6.6                  |
| 4          | 2.6                    | 59                 | 59           | 9.2     | 8.5                  | 8.1                  |
| 5          | 2.0                    | 66                 | 66           | 8.7     | 7                    | 7                    |
| average    |                        | 63 ± 6             | 62 ± 7       | 6.6 ± 2 | 6.5 ± 3 <sup>a</sup> | 6.8 ± 3 <sup>a</sup> |

<sup>a</sup> Unknowns 1 and 2 (see text). Quantification is based on an FID response for compounds with the formula C<sub>7</sub>H<sub>14</sub>O, corresponding to 2-propylcyclobutanol and 2-ethylcyclopentanol.

SCHEME 2. Different Channels of Reactivity from the Triplet State of *n*-Heptanal (box) Showing the Transition Structures and Relative Energies (in kcal/mol), Including Those of the Triplet Biradicals Generated after  $\gamma$ -H and  $\delta$ -H AbstractionTABLE 2. Summary of Heptanal Photolysis Studies<sup>a</sup>

| study                       | wavelength range, $\lambda_{\max}$ (nm) | total pressure (Torr); [initial aldehyde] (ppm) | product yields per molecule of heptanal photolyzed (%) |   |  |                       |
|-----------------------------|---|---|--|---|--|-----------------------|
|                             |   |   | Norrish I. HCO + C <sub>6</sub> H <sub>13</sub>        | Norrish II. pentene + C <sub>2</sub> H <sub>4</sub> O | Norrish II. C <sub>7</sub> H <sub>14</sub> O cyclic alcohols | CO + <i>n</i> -hexane |
| this work, exptl            | 275–380, 312 <sup>b</sup>               | 755; 2.0–2.9                                    | 1-hexanol: trace, <0.5, hexanal: 7 ± 2                 | 63 ± 7  | possible ID <sup>f</sup> ; 14 ± 7%                           | 0 <sup>j</sup>        |
| this work, theor            | –                                       | –   | <1   | ≤80 <sup>e</sup>                                      | ≥20 <sup>g</sup>   | 0                     |
| Tadić et al. <sup>13a</sup> | 275–380, 313 <sup>b</sup>               | 700; 100  | CO: 10 ± 8   | 38 ± 3  | not observed <sup>h</sup>                                    | 0                     |
| Tang and Zhu <sup>14</sup>  | 308, 308 <sup>c</sup>                   | 300; 1700–13000                                 | HCO: 15 ± 7 <sup>d</sup>                               | 27 ± 3  | 40 ± 4 <sup>i</sup>  | 23 ± 9                |

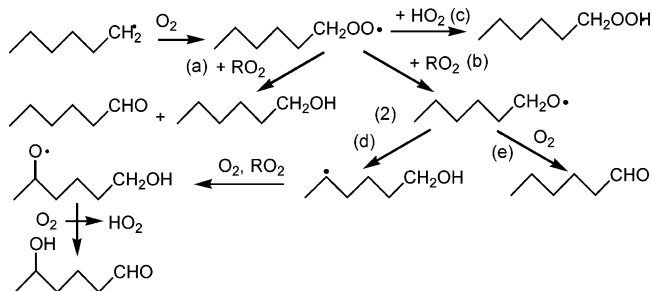
<sup>a</sup> Total quantum yield for all channels was reported as 0.31 ± 0.01. <sup>b</sup> TL-12 UV fluorescent bulb light source.  $\lambda_{\max}$  does not include the narrow spikes at 320 nm and other wavelengths. <sup>c</sup> Excimer laser light source. Tang and Zhu measured HCO over the range 280–330 nm and other products at 308 nm only. <sup>d</sup> At 310 nm. By 315 nm, the yield had dropped to 10%. <sup>e</sup> Corresponds to the formation of the biradical <sup>3</sup>BR- $\gamma$ , which can partition to cyclobutanol and 1-pentene + C<sub>2</sub>H<sub>4</sub>O and undergo disproportionation reactions, assuming irreversibility. <sup>f</sup> Two peaks, each with yields of about 7%, were observed that may be cyclic alcohols (see text). <sup>g</sup> Corresponds to the formation of the biradical <sup>3</sup>BR- $\delta$ , which can cyclize to form cyclopentanol, assuming irreversibility. <sup>h</sup> Using Fourier transform infrared spectroscopy (FTIR). Tang and Zhu<sup>14</sup> suggest they were not observed because parent aldehyde absorption peaks overlap those of cyclic alcohols. <sup>i</sup> Using MS only (no GC). Identification should be considered tentative (see text). <sup>j</sup> No hexane was observed in the GC-FID or SPME/GC-MS analyses (also see text).

**Type II Channels.** The hydrogen abstraction channels (b and c, Scheme 1 and Scheme 2) can result in either C<sub>7</sub> cyclic alcohols or decomposition products. All experimental studies observe substantial amounts of pentene and acetaldehyde, although reported yields range from 27 to 63%.

Our result, 63 ± 7%, is based on a measurement of both 1-pentene and acetaldehyde, both of which are easily and reliably quantified via GC-FID and GC-MS. Our yields of 1-pentene and acetaldehyde are in excellent agreement with one another (Figure 1). The only source of a positive artifact for this measurement is decomposition of an unknown compound

to produce acetaldehyde and 1-pentene in the column. Although this cannot be completely ruled out, such a labile source compound is not known.

Both Tadić et al.<sup>13</sup> and Tang and Zhu<sup>14</sup> quantified 1-pentene and hydroxyethene and/or acetaldehyde using FTIR but noted that quantification of each of these products with FTIR is complicated by the overlap of most of their absorptions with heptanal. Tadić et al.<sup>13</sup> assigned a 38 ± 3% yield to the Norrish II decomposition channel on the basis of 1-pentene, for which they used a weak absorption peak that did not overlap with heptanal, and Tang and Zhu<sup>14</sup> assigned a yield of 27 ± 3% but

**SCHEME 3. Expected Reaction Pathways Available to the Hexyl Radical under NO<sub>x</sub>-Free Atmospheric Conditions**


did not specify which products were used to derive this value. A possible source of negative artifacts for these measurements is reactions with OH or other radicals that may be more important at the higher reactant concentrations used in these studies.

Our theoretical results indicate that there is potential for 1-pentene and hydroxyethene to be the predominant products, as the  $\gamma$ -H abstraction pathway is favored; however, the resulting biradical can either decompose or cyclize. It must also be noted that the theoretical percentages in Table 1 correspond to generation of the biradicals, which can undergo further reactions and undergo a reversible process<sup>22</sup> in the gas phase.

**Formation of Cyclic Alcohols.** From a theoretical point of view, a yield of cyclic alcohols of 20% is expected from the  $\delta$ -H abstraction pathway, and additional cyclic alcohols are expected from the  $\gamma$ -H abstraction pathway, assuming an irreversible pathway following biradical generation.<sup>22</sup> Tadić et al.<sup>13</sup> postulated that cyclic alcohols were likely products of heptanal photolysis but could not observe them with FTIR. Tang and Zhu et al.<sup>14</sup> estimated a yield for cyclic alcohols of 40% using a residual gas analyzer to identify fragment ions that could arise from cyclic alcohols. Given the complexity of the organics in their experiments and the lack of authentic standards, however, quantification is difficult with this method. Our experimental evidence, together with the other studies, indicates that yields of cyclic alcohols fall in the 15–30% range, bracketed by the observation of likely peaks in our chromatograms at the low end and the yields of other products, which account for most of the carbon, at the upper end.

**Decarbonylation.** We observe no evidence for a channel producing CO and hexane (d, Scheme 1) in either of our theoretical or experimental results. No traces of hexane were observed in the GC-FID or SPME/GC-MS samples. Our detection limit for *n*-hexane corresponds to a yield of about 0.1%. From an energetic point of view, it is known that the experimentally observed activation energy for H–CO dissociation to CO and atomic hydrogen (path c in Scheme 1) is relatively high, 15.8 kcal/mol,<sup>23</sup> thus making such a process rather unfavorable. Similarly, radical pair recombination, although thermodynamically more advantageous, cannot compete with the radical reactions with molecular oxygen.

Tadić et al.<sup>13</sup> also found no evidence for decarbonylation. Tang and Zhu,<sup>14</sup> on the other hand, assigned a large yield based on FTIR measurements of CO, from which they subtracted HCO measurements obtained with cavity ring down, assigning this

to the Norrish II decomposition channel. They could not detect hexane with FTIR because of overlap with heptanal and did not observe evidence for it with MS. As it seems unlikely that decarbonylation is an accessible pathway for photoexcited heptanal, it is possible that the other secondary sources of CO become very significant at the high concentrations used by Tang and Zhu<sup>14</sup> in their experiments.

**Experimental Section**

**Chamber Experiments.** Very similar experiments have been described in detail elsewhere<sup>24,25</sup> and are only briefly outlined here. Investigations of heptanal photolysis were performed in a 240 (experiments 1–3) or 1200 L (experiments 4 and 5) collapsible Teflon reaction chamber (200 mil) at  $296 \pm 2$  K and atmospheric pressure. The large chamber was equipped with a Teflon mixing fan (used while the chamber was filled), and both chambers were surrounded by eight fluorescent UVB lamps (275–380 nm,  $\lambda_{\text{max}} = 312$  nm). In our chamber configuration, these lamps result in a heptanal photolysis rate of  $(1.65 \pm 0.03) \times 10^{-5} \text{ s}^{-1}$ .

A small quantity of heptanal (purity 95%, used as received) was slowly introduced into the chamber by evaporating it into the purified air used to fill the chamber. Gas samples were automatically collected from the chamber every 23 min and introduced, via a 2 mL sampling loop, into a GC-FID, equipped with a capillary column (DB-1, 0.32 mm ID, 3  $\mu\text{m}$  film, 30 m), programmed to 2 min at  $-50$  °C, then 14 °C/min to 170 °C. The GC-FID was calibrated with a cyclohexane standard. Effective carbon numbers<sup>26</sup> normalized to the cyclohexane calibration were measured in our laboratory and were used to calculate concentrations of hydrocarbons and carbonyl compounds, as follows: hexanol 5.6, acetaldehyde 1.02, 1-pentene 5.0, heptanal 6.15, and hexanal 5.15.<sup>27</sup> Concentrations and yields derived with this method have overall uncertainties of  $\pm 10\%$  (aliphatics) and  $\pm 15\%$  (oxygenates). Relative errors for a set of reactants and products normalized to the same calibration standard are about  $\pm 5\%$  and  $\pm 10\%$ , respectively.

The chamber was also sampled with SPME/GC-MS<sup>25</sup> before and after each experiment. Used this way, SPME provides qualitative mass spectral information. Experiments were also monitored for the production of organic acids using in-inlet derivatization/GC-MS,<sup>24</sup> but no acid formation was observed.

**Quantum Mechanical and Chemical Kinetics Methods.** Quantum mechanical calculations were carried out using the Gaussian 03 suite of programs.<sup>28</sup> Density functional theory at the

(24) Orzechowska, G. E.; Nguyen, H. T.; Paulson, S. E. *J. Phys. Chem. A* **2005**, *109*, 5366–5375.

(25) Orzechowska, G. E.; Paulson, S. E. *J. Phys. Chem. A* **2005**, *109*, 5358–5365.

(26) Scanlon, J. T.; Willis, D. E. *J. Chromatogr. Sci.* **1985**, 333–340.

(27) Paulson, S. E.; Meller, R.; Chung, M.; Kramp, F. *Final Report: Total nonmethane organic carbon: Development and validation of a new instrument, and measurements of total nonmethane organic carbon and C2–C7 hydrocarbons in the south coast air basin*; California Air Resources Board Report No. 95-335, 1999.

(28) Frisch, M. J.; Trucks, G. W.; Schlegel, H. B.; Scuseria, G. E.; Robb, M. A.; Cheeseman, J. R.; Montgomery, J. A., Jr.; Vreven, T.; Kudin, K. N.; Burant, J. C.; Millam, J. M.; Iyengar, S. S.; Tomasi, J.; Barone, V.; Mennucci, B.; Cossi, M.; Scalmani, G.; Rega, N.; Petersson, G. A.; Nakatsuji, H.; Hada, M.; Ehara, M.; Toyota, K.; Fukuda, K.; Hasegawa, J.; Ishida, M.; Nakajima, T.; Honda, Y.; Kitao, O.; Nakai, H.; Klene, M.; Li, X.; Knox, J. E.; Hratchian, H. P.; Cross, J. B.; Bakken, V.; Adamo, C.; Jaramillo, J.; Gomperts, R.; Stratmann, R. E.; Yazyev, O.; Austin, A. J.; Cammi, R.; Pomelli, C.; Ochterski, J. W.; Ayala, P. Y.; Morokuma, K.; Voth, G. A.; Salvador, P.; Dannenberg, J. J.; Zakrzewski, V. G.; Dapprich, S.; Daniels, A. D.; Strain, M. C.; Farkas, O.; Malick, D. K.; Rabuck, A. D.; Raghavachari, K.; Foresman, J. B.; Ortiz, J. V.; Cui, Q.; Baboul, A. G.; Clifford, S.; Cioslowski, J.; Stefanov, B. B.; Liu, G.; Liashenko, A.; Piskorz, P.; Komaromi, I.; Martin, R. L.; Fox, D. J.; Keith, T.; Al-Laham, M. A.; Peng, C. Y.; Nanayakkara, A.; Challacombe, M.; Gill, P. M. W.; Johnson, B.; Chen, W.; Wong, M. W.; Gonzalez, C.; Pople, J. A. *Gaussian 03*, revision C.02; Gaussian, Inc.: Wallingford, CT, 2004.

(22) Turro, N. J. *Modern Molecular Photochemistry*; University Science Books: Sausalito, 1991.

(23) Krasnoperov, L. N.; Chesnokov, E. N.; Stark, H.; Ravishankara, A. R. *J. Phys. Chem. A* **2004**, *108*, 11526–11536.

UB3LYP/6-31G\* level of theory was used to obtain structure and energetic information along the triplet state reaction coordinate.<sup>29–31</sup> All relative energies reported are inclusive of the scaled zero-point energy (ZPE).<sup>32</sup> Vibrational frequency calculations were also used to confirm that minimum energy structures have no imaginary frequencies, and transition structures (TS) have the appropriate imaginary frequency for  $\alpha$ -cleavage (type I) or H-abstraction (type II).

Chemical kinetics calculations were performed by solving the set of ordinary differential equations describing heptanal photolysis and subsequent reactions of alkyl, alkyl peroxy, and alkoxy radicals together with other products, relevant inorganic reactions, and physical loss processes, using the software package FACSIMILE (AEA Tech., U.K.). Reaction rate constants were obtained from the evaluations by Sander et al.<sup>33</sup> and Lightfoot et al.<sup>34</sup>

**Acknowledgment.** We thank Prof. Jochen Stutz for measuring the emission spectrum of the UV lamps and Dr. Zsuzsanna

(29) Becke, A. D. *J. Chem. Phys.* **1993**, *98*, 5648–5652.

(30) Krishnan, R.; Binkley, J. S.; Seeger, R.; Pople, J. A. *J. Chem. Phys.* **1980**, *72*, 650–654.

(31) Head-Gordon, M.; Pople, J. A. *Chem. Phys. Lett.* **1988**, *153*, 503–506.

Marka and Prof. Miguel A. Garcia-Garibay for valuable discussions. This work was supported by the National Science Foundation under Grants ATM-0100823 and CHE-0240203. L.M.C. thanks the National Science Foundation, the Paul and Daisy Soros Fellowship, and the NSF IGERT: Materials Creation Training Program (MCTP) (Grant number: DGE-0114443) for graduate support.

**Supporting Information Available:** Cartesian coordinates of the stationary points. This material is available free of charge via the Internet at <http://pubs.acs.org>.

JO060596U

(32) Scott, A. P.; Radom, L. *J. Phys. Chem.* **1996**, *100*, 16502–16513.

(33) Sander, S. P.; Friedl, R. R.; Golden, D. M.; Kurylo, M. J.; Huie, R. E.; Orkin, V. L.; Moortgat, G. K.; Ravishankara, A. R.; Kolb, C. E.; Molina, M. J.; Finlayson-Pitts, B. J. *Kinetics and Photochemical Data for use in Atmospheric Studies, Evaluation #14*; Jet Propulsion Laboratory Publication 02-25, 2002.

(34) Lightfoot, P. D.; Cox, R. A.; Crowley, J. N.; Destriau, M.; Hayman, G. D.; Jenkin, M. E.; Moortgat, G. K.; Zabel, F. *Atmos. Environ.* **1992**, *26A*, 1805–1961.